

Original Research

Optimization Study on the Control Effect of Rainwater Runoff in Extensive Green Roof Based on Response Surface Methodology

Xiaohui Fu^{1,2*}, Hui Wang^{1,2}, Mengxuan Yu^{1,2}, Nan Liang^{1,2}, Hao Zhang³, Xinyu Qi¹

¹College of Civil Engineering and Architecture, Anhui Polytechnic University, Wuhu 241000, China

²Wuhu Green Building and Intelligent Construction Engineering Technology Research Center, Wuhu 241000, China

³Gold Mantis School of Architecture, Soochow University, Suzhou 210098, China

Received: 12 January 2023

Accepted: 7 March 2023

Abstract

To renovate an ordinary building roof into an extensive green roof (GR), on the basis of optimizing the runoff process, the total runoff control rate (TR-CR) and peak runoff control rate (PR-CR) were analyzed with the SWMM model under parameter sensitivity analysis. The response surface method (RSM) was used to investigate the effect of area ratio (GR area to total roof area), width (surface width per unit), and soil hydraulic conductivity on TR-CR and PR-CR. The optimal test conditions were obtained through the establishment of quadratic regression equations. The results showed that the effects of the three factors on TR-CR were in the order of area ratio>hydraulic conductivity>width, and on PR-CR was area ratio>width>hydraulic conductivity. Considering the volume capture ratio (80%) of annual rainfall and construction cost of the GR, under the optimal conditions of the area ratio of 0.79, width of 2.21 m, and hydraulic conductivity of 55.59 mm/h, the average values of TR-CR and PR-CR for this optimization scheme were 80.2% and 80.9%, respectively. This result show that the multiple quadratic regression model established is reliable. Therefore, the RSM can effectively optimize the simulation parameters, and provide some theoretical and practical basis for the renovation or construction of GRs.

Keywords: extensive green roof, rainwater runoff, parameter optimization, response surface method, SWMM

Introduction

In recent years, with the rapid development of urbanization, the proportion of impervious surface areas has increased dramatically, which has led to a series of

urbanization hydrological and environmental problems, such as the “heat island effect”, “rain island effect”, and rainfall flooding problems, and especially the rain flood problem is most prominent [1-3]. These problems can be effectively solved by adopting new stormwater management strategies, such as the concept of sponge city construction [4-5]. There are many types of low-impact development (LID) techniques for sponge cities, such as permeable pavements, green roofs, sunken

*e-mail: fuxiaohui@ahpu.edu.cn

green spaces, and bioretention facilities, et al [6]. The GR is one of the vital technical methods of sponge city construction, which mainly consists of a surface layer, soil layer, and drainage layer, which is a planting soil laid on the roof and then planted with green plants [7]. Rainwater can be retained in the plants and soil, thus delaying rainwater's total runoff and peak runoff into the sewers [8]. It reduces the pressure on the drainage network during peak periods, thus reducing the risk of flooding, with better economic, ecological and social benefits.

According to the depth of the planting substrate (mainly composed of soil layer), the complexity of the landscape, and the number of optional plants, GRs can be divided into extensive GRs and intensive GRs, also known as simple GRs and garden GRs [9]. When the building is restricted by the load of the roof itself or other factors, intensive GRs cannot be designed, but extensive GR can be designed. Extensive GRs are green roofs with a substrate depth of generally no more than 150mm, usually using drought-tolerant lawns, ground covers, shrubs or creepable climbers for green roof coverings [10]. Because of the thinner substrate and lower maintenance and management costs, it has better application prospects than intensive GRs.

Many studies have shown that the rainwater retention effect of GRs is the key to their ability to effectively delay the time of flow production and reduce the total amount of runoff [11-12]. The rainwater retention capacity of GRs mainly depends on the rainwater absorption capacity of the soil layer [13]. The plants in the surface layer also have some interception effect on rainwater [14]. In contrast, the evapotranspiration water consumption of plants in the surface layer is key to maintaining the substrate layer's rainwater absorption capacity [15-16]. Stovin et al. [17] concluded that the change of soil water content in the soil layer due to plant evapotranspiration significantly impacts the change in soil water content due to plant evapotranspiration on the total runoff reduction and cannot be ignored.

Most existing studies are based on empirical equations of soil infiltration (Horton, Kostikov equation, etc.) or Richards' theoretical equations to study the rainfall-runoff process of GRs by simulating soil infiltration in the soil layer [18-20]. Related

modeling software includes SWMM, Hydrus-1D, etc., which involve the influence of many parameters such as GR site parameters, physical properties and depth of soil, vegetation types, and seasonal changes, and the solution process is complicated [21-22].

In this paper, based on the renovation of an ordinary building roof into a GR, we take the characteristics of rainfall-runoff and retention of GRs to screen out the sensitive factors such as area ratio, width, and soil hydraulic conductivity from the main factors that affecting the GR runoff process. The effect of area ratio, width, and hydraulic conductivity on the TR-CR and PR-CR was optimized by RSM. This study developed a dynamic simulation method of the GR rainfall-runoff process, and provide some theoretical and practical basis for the renovation or construction of GRs.

Methodology

Site Description

The study has been carried out at Anhui Polytechnic University, Wuhu City (Anhui Province, China). The city of Wuhu is located in eastern China and has a humid temperate subtropical climate with hot and muggy summers, cold winters, and an average rainfall of 1100-1300 mm/year [23]. For the implementation purpose, teaching building C (31.338822°N, 118.411518°E) has been selected to simulate the hypothetical GR scenario (Fig. 1).

The experimental site is the C# building of the university, which is used for office, teaching and experimentation. It occupies about 2885 m² of an existing flat roof with a slope of 2.0%, which is only equipped with solar panels. This condition often resulted in minor flooding on the campus during heavy rains. Therefore, the study's main purpose is to evaluate the hydrologic performance by changing this roof to a green one for runoff volume and peak runoff reduction.

GR Simulations in SWMM

The SWMM model is developed by the US Environmental Protection Agency and is most



Fig. 1. Study area map of teaching building C. a) Area map of location; b) Area map of the SWMM model.

commonly used to simulate single or long-term rainfall events generated by different basins. SWMM is a rainfall-runoff model based on hydrology-hydraulic and water quality simulation of given rainfall data. In the version of SWMM5.0, LID modules are added, and GR emulation has been equipped in LID modules since version 5.1 in 2014. In the latest version of SWMM5.2.0, eight common LID modules include the bio-retention cell, rain garden, GR, infiltration trench, permeable pavement, rain barrel, rooftop disconnection, and vegetative swale. Through the modeling of water processes, such as retention, evaporation, and infiltration, combining the hydraulic modules of SWMM, the process of sub-catchment runoff and LID performance can be achieved easily. By changing the parameters of different LID facilities, such as surface, soil, storage, and drain, a better rainwater control effect can be obtained.

LID modules are generally defined and assigned to sub-catchments with three different LID editor forms: 1) the control editor, 2) the group editor, and 3) the usage editor [24]. Take GR for example, the LID control editor aims to define GR types from eight different LID types that can be applied in the LID group editor to add GR types in the established sub-catchments. The usage editor is aimed to explain how the GR types are deployed in the group's sub-catchments from the LID group [24].

Based on the above analyses, the structure of the GR is mainly divided into three layers: surface layer, soil layer, and drainage mat. Considering the runoff bearing capacity of the roof, the lawn block or lawn roll material is preliminarily selected on the surface layer, and the thickness is about about 20-30 mm. Because the total porosity of the pastoral soil is minor and the drainage rate is slow, the soil layer uses improved soil [25]. The main ingredients are pastoral soil, lightweight aggregate, peat, humus soil, and vermiculite. The weight ratio of 1:1:1:1:0.5, which have better drainage rates [26]. The user's manual of SWMM stipulates that the soil depth of an extensive GR is generally not greater than 150 mm, so the soil depth of a GR is 150 mm, and the material of the drainage mat adopts concave-convex drainage plate, mainly made of polyethylene.

Parameters Simulation and Optimization Design

Parameter Sensitivity

The parameters affecting the output results of GR in the SWMM model are mainly divided into two categories: one is the parameter of the surface runoff and infiltration about sub-catchments, and the other is the parameter related to GR [27]. To investigate the influence of different input parameters on the model's output, a sensitivity analysis and optimization analysis of GR parameters are conducted. In the design process of a GR, the length, the surface width, and the water storage depth are often used as the main design

parameters. Still, the effect of water storage depth on runoff control rate is not apparent in rainfall events with high rainfall intensity. The longitudinal slope is often closely related to the actual engineering elevation [28]. Therefore, the area ratio, width, berm height, vegetation volume fraction, soil thickness, hydraulic conductivity, and manning coefficient of the impervious area (N-imperv) were selected for sensitivity analysis.

This paper examined the effect of GR parameters on runoff control capacity by varying the GR design parameters through the SWMM model. The sensitivity coefficients are usually used to respond to the influence of GR parameters on the model output values, and the sensitivity coefficients are shown in Equation (1) [29].

$$SC = \frac{\Delta B/B}{\Delta A/A} \quad (1)$$

Where SC is the sensitivity coefficient, ΔB is the variation of the model output value, B is the model output value, ΔA is the variation of the model input value, and A is the model input value.

Single Factor

In this study, the TR-CR and the PR-CR were selected as evaluation indexes to investigate the parameter settings that affect the runoff control of GR and thus the optimization of the main influencing parameters. From the simulated parameters of the GR, it could be seen that the sensitivity coefficients of the area ratio, the width, and the hydraulic conductivity are higher than the berm height, the vegetation volume, the fraction surface roughness, the soil thickness, and the N-imperv area. Thus, the area ratio, width, and hydraulic conductivity were selected as the three main factors to conduct single factor and RSM analysis.

RSM Design

The RSM was used to study the effects of area ratio (A), width (B), and hydraulic conductivity (C) on the TR-CR and PR-CR. The experiments were conducted according to the Box-Behnken experimental scheme of Design Expert software. According to the material properties of the improved soil, the area ratios were set as 0.70, 0.82, and 0.95, the width was set as 0.50, 3.25, and 6 m, and hydraulic conductivity were set as 5, 32.5, and 60 mm/h, respectively (Table 1).

Input Data

The rainfall data used in the simulation parameter optimization process were derived from the Chicago rain type. The rainfall data used in the calibration and validation process were collected from the China Meteorological Administration. The sub-catchment area and the slope in the model were field measurements. Runoff volume was measured using a weight-based

Table 1. Design of the response surface factors and levels.

Factors		Level		
		-1	0	+1
A	Area ratio	0.70	0.82	0.95
B	Width (m)	0.50	3.25	6
C	Hydraulic conductivity (mm/h)	5	32.5	60

system from a rain canal downstream of the drainage outlets [24]. Other model parameters refer to relevant research results and the SWMM user manual.

Calibration and Validation Procedures

The commonly used model calibration process is as follows. Firstly, in the same coordinate system plot the curve of simulation results and the actual monitoring results. Then continuously adjust the model sensitive parameters until the two curves are the closest, and stop adjusting the sensitivity parameters finally [30]. The model results obtained at this condition are closest to the actual results, and the model parameter rate is then completed. Usually, the Nash-Sutcliffe efficiency index (NSE) is chosen as the evaluation index of the model accuracy widely in reproducing the runoff flow on an event basis, and when $NSE > 0.75$, the simulation results can be considered to be in good agreement with the actual monitoring data, and the model performance is good [30]. Which, the NSE was expressed by Equation (2) [31]:

$$NSE = 1 - \frac{\sum_{i=1}^n (Q_{i-SV} - Q_{i-MV})^2}{\sum_{i=1}^n (Q_{i-MV} - Q_{i-MMV})^2} \quad (2)$$

where SV is the simulated values, MV is the measured values, MMV is the mean measured values, n is the number of simulated or measured values.

Results and Discussion

Calibration and Validation Results

Simulations in the current roof without LID modules are used to calibrate the model. The curves of measured flow (recorded every 6 minutes) and simulated flow can be seen in Fig. 2. The simulation results showed that the SWMM model had a good performance. The value of NSE was 0.83, which was greater than 0.75. The peak of the monitoring liquid level and simulation liquid level were 0.23 m and 0.20 m. The NSE value indicated that the model could generate the duration and amplitude of peak flow. The simulated curve was in good agreement with the measured curve.

Parameter Sensitivity Analysis

The sensitivity analysis of this model parameter is based on a single rainfall event. It analyzed the sensitivity coefficients of the area ratio, width, berm height, vegetation volume, fraction surface roughness, soil thickness, hydraulic conductivity, and N-imperv. It could be seen that the area ratio had the most significant influence on the TR-CR and PR-CR with sensitivity coefficients of -0.909 and -0.882, respectively (Fig. 3). The sensitivity coefficients of width were 0.635 and 0.721, which ranked third and second, respectively. The sensitivity coefficients of hydraulic conductivity in total runoff and peak runoff were -0.835 and -0.680, which ranked second and third, respectively. Based on the above sensitivity coefficient analysis, the area ratio,

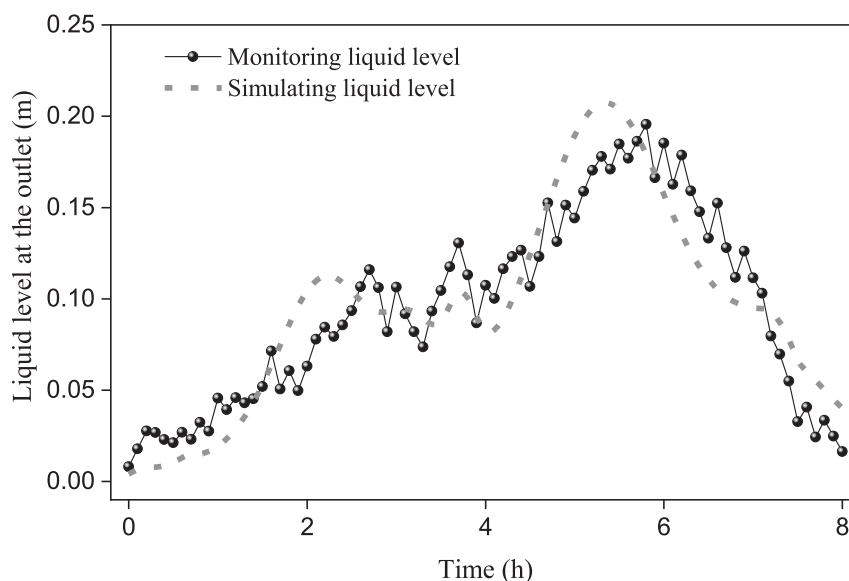


Fig. 2. Comparison of simulated runoff and monitored runoff (rainfall event in 16/03/2022).

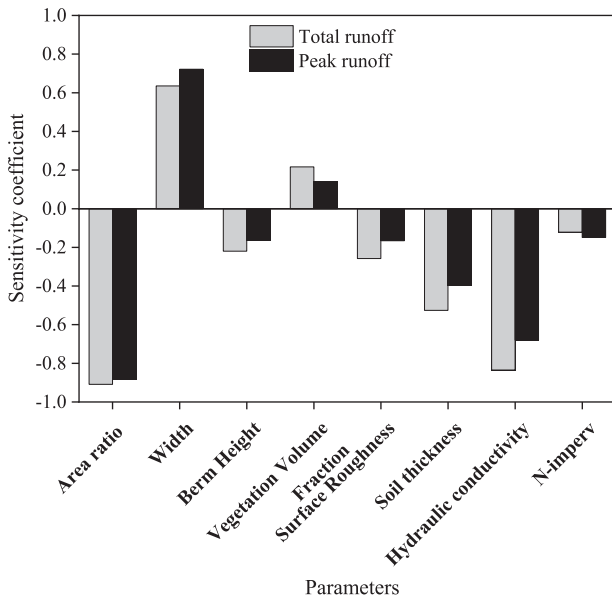


Fig. 3. Parameter sensitivity coefficients of GR model.

width, and hydraulic conductivity were selected as the main parameters to conduct RSM analysis.

Single Factor Analysis

The commonly used rainfall return period in Wuhu City is 2~3 years. The SWMM model in this study performed rainfall time series with a rainfall return period of 3a. As can be seen from Fig. 4a), the TR-CR

and PR-CR both increased with the increase of the area ratio. The Technical Specification for Planted Roofs stipulates that the ratio of GR area to total roof area should be more than 80% in extensive GR type [32]. Nonetheless, for the consideration of load bearing and cost, combined with the TR-CR and PR-CR, the area ratio in this study was taken in the range of 70%-95%.

The runoff control rate is most remarkable at a width of 0.5 m (Fig. 4b). Both the TR-CR and PR-CR decreased as the width increased, with the TR-CR decreasing more than the PR-CR. With the increase in width, the runoff time will decrease, thus the control rate will decrease as the width here corresponds to the characteristic width of the catchment area [33]. Combined with the relevant design codes, the widths in this study ranged from 0.5 m to 6.0 m. The TR-CR and PR-CR increased with the increase in soil hydraulic conductivity (Fig. 4c). Considering different soil types such as commonly used field soils, improved soils, and inorganic planting soils, combined with the TR-CR and PR-CR, the range of soil hydraulic conductivity is 5.0 mm/h to 50.0 mm/h regarding the SWMM user manual and related specifications.

Response Surface Analysis

The TR-CR and PR-CR were used as evaluation indexes, and 17 working conditions were designed according to the Box-Behnken response surface of the three single factors and three levels (Table 1). The TR-CR and PR-CR of GR were calculated by

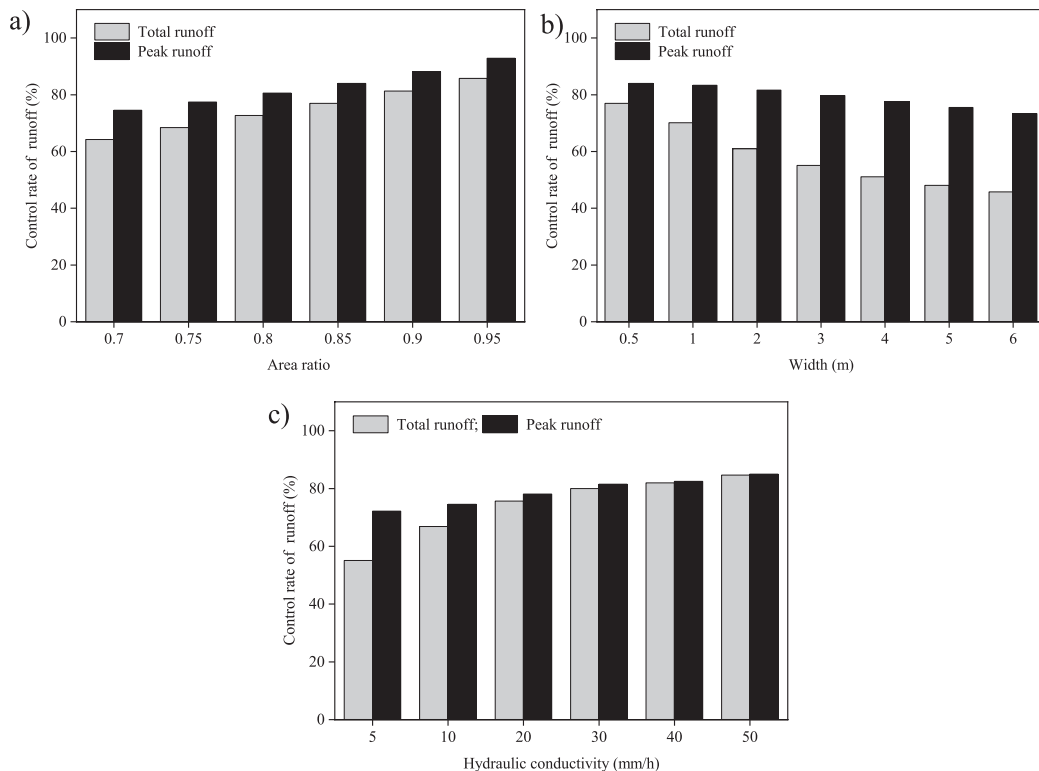


Fig. 4. Single factor analysis of area ratio, width and hydraulic conductivity.

substituting 17 working conditions into the SWMM model and performing simulations. The response surface test and simulation results are shown in Table 2. The TR-CR and PR-CR in each experimental condition have some similarities. When the area ratio was 0.70, both TR-CR and PR-CR were relatively low. The highest removal rate of TR-CR (94.8%) and PR-CR (93.9%) both occurred in working condition 4 ($A = 0.95$, $B = 0.5$ m, $C = 32.50$ mm/h), which was also similar to the best working condition in the latter classification. Relative to the other two area ratios, TR-CR and PR-CR are higher when the area ratio is 0.95. The water storage capacity of the soil material is lower when the area ratio is smaller, which subsequently affects the control of water quality and quantity of the GR. The effect of width on TR-CR and PR-CR is relatively tiny compared to area ratio and hydraulic conductivity. The TR-CR and PR-CR are relatively high because rainwater's better permeability when the hydraulic conductivity is higher.

Construction of Response Surface Model and Significance Test

According to the experimental results, the TR-CR (Y1) and PR-CR (Y2) were simulated by equations using Design Expert, and the results were subjected to

ANOVA. Then the significance tests were conducted for each factor using F-values, specifying that $p < 0.05$ when the model was significant, and the resulting multiple quadratic regression equation was shown as follows.

$$Y1 = 79.61 + 10.46A - 5.71B + 13.41C - 0.12AB + 1.38AC + 6.98BC - 1.32A^2 + 2.01B^2 - 10.58C^2 \quad (3)$$

The positive coefficients of the variables A and C in Equation (3) indicated that they both cause an increase in the response value, and the negative quadratic term coefficients suggested that they have extreme value points and are capable of optimal analysis [34]. The F-value of the model was 33.21, $p < 0.0001$, the signal-to-noise ratio was 20.356, much more significant than 5, and the Adj R^2 of the model was 0.9477, indicating that the model conformed well to reality (Table 3). The correlation coefficient of the regression model R^2 was 0.9771, which is close to 1, meaning that the empirical model can reflect the experimental data better and the experimental error was more minor, which can predict the actual condition. T-test showed that $p < 0.0001$ for A, and C and $p = 0.0018$ for B, indicating that A and C significantly affected the results than B, which was consistent with the previous conclusion.

Table 2. Experimental design and removal rate analysis.

Condition No.	Actual value			Code value			Total average removal rate/%	
	Area ratio	Width (m)	Hydraulic conductivity (mm/h)	Area ratio	Width (m)	Hydraulic conductivity (mm/h)	TR-CR (%)	PR-CR (%)
1	0.82	0.50	60.00	0	-1	1	83.8	83.8
2	0.95	3.25	60.00	1	0	1	94.1	93.2
3	0.95	6.00	32.50	1	1	0	88.0	89.7
4	0.95	0.50	32.50	1	-1	0	94.8	93.9
5	0.82	3.25	32.50	0	0	0	79.6	81.7
6	0.70	3.25	60.00	-1	0	1	71.7	72.9
7	0.82	3.25	32.50	0	0	0	79.6	81.7
8	0.82	3.25	32.50	0	0	0	79.6	81.7
9	0.82	0.50	5.00	0	-1	-1	74.6	83.0
10	0.82	6.00	5.00	0	1	-1	44.3	71.4
11	0.70	0.50	32.50	-1	-1	0	72.4	73.2
12	0.70	6.00	32.50	-1	1	0	66.1	70.3
13	0.82	3.25	32.50	0	0	0	79.6	81.7
14	0.82	6.00	60.00	0	1	1	81.5	81.9
15	0.82	3.25	32.50	0	0	0	79.6	81.7
16	0.70	3.25	5.00	-1	0	-1	44.1	68.5
17	0.95	3.25	5.00	1	0	-1	60.9	87.1

Table 3. Response surface model results and significance analysis.

Variables	Square and		Degree of freedom		Mean Square		F-value		P-value	
	Y1	Y2	Y1	Y2	Y1	Y2	Y1	Y2	Y1	Y2
Models	3271.56	926.08	9	9	363.51	102.90	33.21	137.29	<0.0001***	<0.0001***
A	875.25	778.64	1	1	875.25	778.64	79.95	1038.92	<0.0001***	<0.0001***
B	261.09	52.72	1	1	261.09	52.72	23.85	70.35	0.0018*	<0.0001***
C	1438.97	59.56	1	1	1438.97	59.56	131.45	79.47	<0.0001***	<0.0001***
AB	0.06	0.42	1	1	0.06	0.42	0.01	0.56	0.9435	0.4804
AC	7.67	0.74	1	1	7.67	0.74	0.70	0.99	0.4302	0.3535
BC	194.90	23.94	1	1	194.90	23.94	17.80	31.94	0.0039*	0.0008**
A ²	7.36	0.22	1	1	7.36	0.22	0.67	0.29	0.4394	0.6049
B ²	16.97	0.13	1	1	16.97	0.13	1.55	0.17	0.2531	0.6912
C ²	471.04	9.71	1	1	471.04	9.71	43.03	12.96	0.0003**	0.0087*
Residuals	76.63	5.25	7	7	10.95	0.75				
Loss of proposed items	76.63	5.25	3	3	25.54	1.75				
Pure Error	0.000	0.000	4	4	0	0				
Total deviation	3348.18	931.32	16	16						

Notes: *significant at P<0.05; **significant at P<0.001; ***significant at P<0.0001.

$$Y_2 = 81.72 + 9.87A - 2.57B + 2.73C - 0.32AB + 0.43AC + 2.45BC + 0.23A^2 - 0.17B^2 - 1.52C^2 \tag{4}$$

Similar to Equation (3), the coefficients of both variables A and C in are positive and can cause an increase in the response value (Equation 4). The positive quadratic term coefficients indicated that they have a minimal value point. The F-value of the model was 137.29 with a p-value<0.0001, and the signal-to-noise ratio was 39.555, much more significant than 5 (Table 3). The Adj R² of the model is 0.9871, which indicated that the empirical model can better reflect the experimental data, and the experimental error is small enough to predict the actual situation. T-test showed that the p-values of Equation (4) for A, B, and C are <0.0001, indicating that the effects of factors A, B, and C on peak runoff control rate were significant.

Response Surface Results and Predictive Analysis

To visualize the effect of area ratio, width, and hydraulic conductivity on the TR-CR and PR-CR, three-dimensional plots and contour plots of the different response values under the interaction of two different factors were made using Design Expert (Fig. 5 and Fig. 6).

Fig. 5a) showed the effect of area ratio and width on the TR-CR when the hydraulic conductivity was 32.50 mm/h. It could be seen that the TR-CR rate increased with the increase of width and area ratio, and

the increase with area ratio was more significant than that with width, which showed that the effect of area ratio is more noticeable compared with width. The TR-CR increased with the increase of area ratio as the rise of area ratio will improve the water storage space of the GR. The TR-CR decreased with the width increases since the catchment length of the GR increases, the catchment time is shortened, and more runoff cannot be infiltrated and overflows directly.

The response surface plot of the area ratio and hydraulic conductivity on the TR-CR at the width of 3.25 m is shown in Fig. 5b). The figure showed that with the increase in area ratio and hydraulic conductivity, the TR-CR also increased gradually. The TR-CR increased faster from 5 to 32.5 mm/h and increased slowly from 32.5 mm/h to 60.00 mm/h. At the area ratio of 0.95 and hydraulic conductivity of 60.00 mm/h, the TR-CR reached the maximum value of 94.8%. The overall increase in TR-CR with increasing hydraulic conductivity is because the more significant hydraulic conductivity allows for increased infiltration, which enables more rainwater to enter the subsurface drainage layer of the GR [35]. The effect of area on the TR-CR is more significant than that of hydraulic conductivity, as can be seen from the gradient of the 3D surface slope of the response surface.

When the area ratio is 0.82, the effects of width and hydraulic conductivity on the TR-CR are shown in Fig. 5c). The TR-CR decreased with the increasing width and increased with increasing hydraulic conductivity. The effect of hydraulic conductivity on

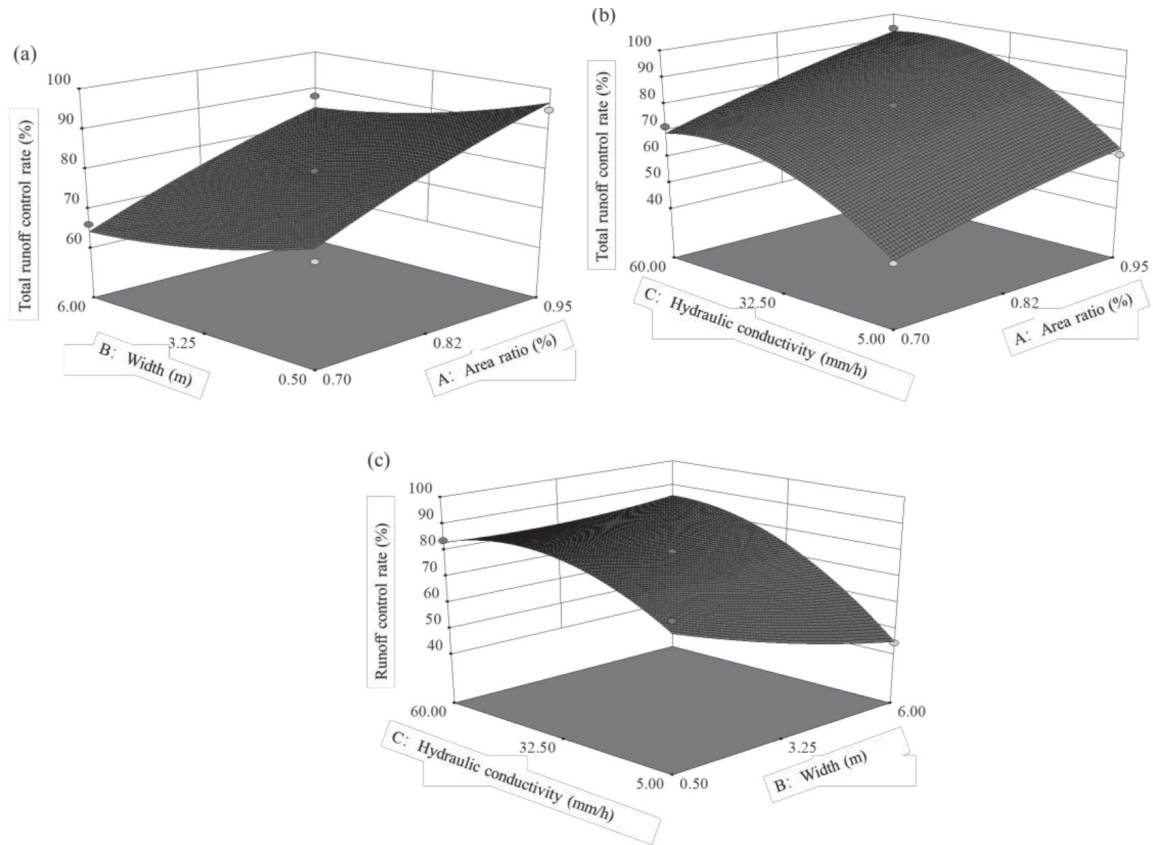


Fig. 5. Contour plot and response surface plot of TR-CR.

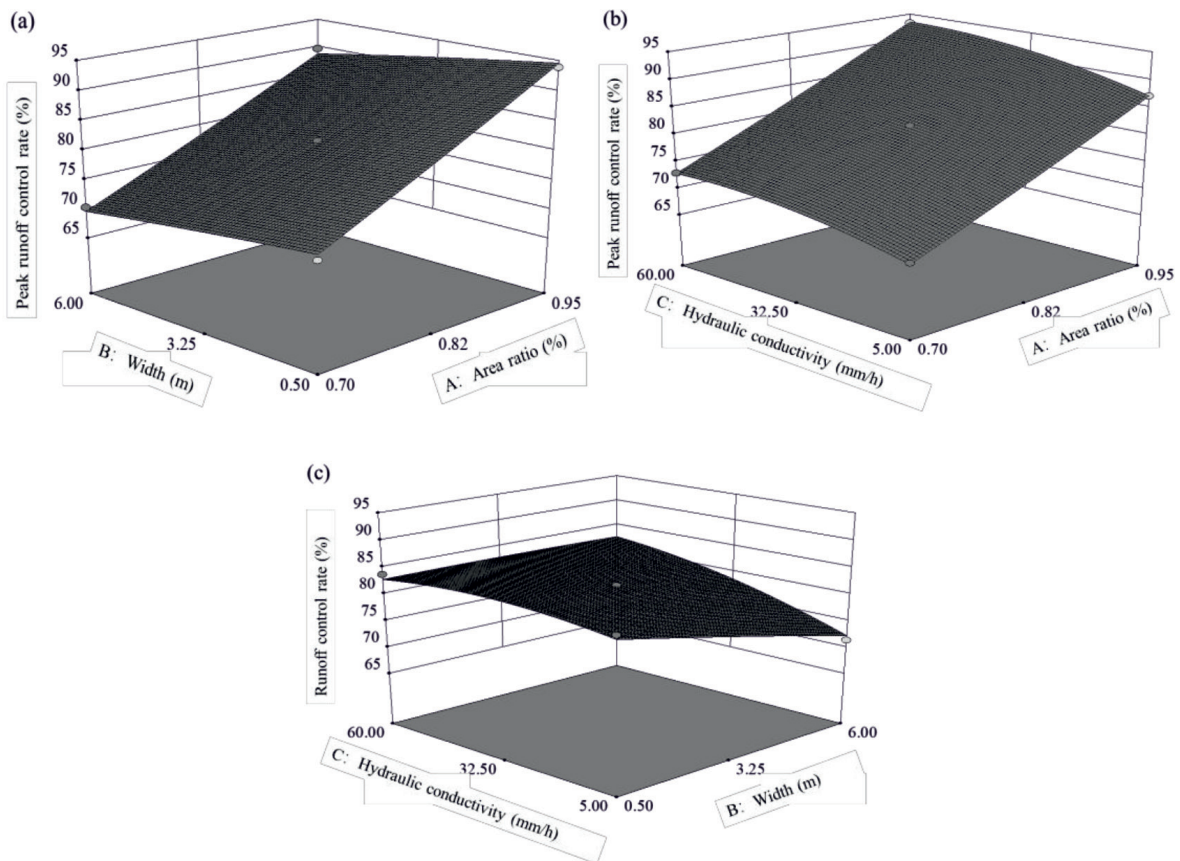


Fig. 6. Contour and response surface of PR-CR.

the TR-CR is more significant than that of width, as can be seen from the gradient of the three-dimensional surface of the response surface. Therefore, it can be analyzed that the three factors affect the TR-CR in the order of area ratio>hydraulic conductivity>width.

Combined with the analysis in Fig. 5, the effect of the area ratio on the PR-CR is the most significant among the three factors, as can be seen from the three-dimensional surface slope in Fig. 6. The area ratio had the greatest effect on PR-CR, and reached the maximum value (93.9%) at the area ratio, width, and hydraulic conductivity of 0.95, 3.25 m, and 60.00 mm/h, respectively (Fig. 6 (a,b)). The effects of width and hydraulic conductivity were relatively less, and the effect of hydraulic conductivity was more significant than that of width on the PR-CR (Fig. 6c). This conclusion is consistent with the analysis in Fig. 5. Therefore, from the three-dimensional surface of the response surface, it can be drawn a conclusion that the order of the effects on the PR-CR is area ratio>width>hydraulic conductivity.

Optimization Validation

The statistical analysis of the daily rainfall of nearly 200 cities in China from 1983 to 2012 in the Technical Guide for Sponge City Construction stipulates the relationship between each city's volume capture ratio of annual rainfall, and its corresponding design rainfall value, respectively [36]. Based on the above data analysis, this guide divides the mainland area of China into five zones. It gives the minimum and maximum limits of each zone's volume capture ratio of annual rainfall. Wuhu City is located in Zone IV, and the volume capture ratio of the annual rainfall of this zone is $70\% \leq \alpha \leq 85\%$. Combined with the geographical situation and construction planning of Wuhu City, the target values of both the TR-CR and the PR-CR of Wuhu City are set to 80%.

In addition to the 80% control target of the TR-CR and the PR-CR, selecting the cost as the secondary control index for further screening. From the optimization solutions, when the area ratio is 0.79, the width is 2.21 m, and the hydraulic conductivity is 55.59 mm/h, the solution is the most suitable, and the TR-CR and PR-CR are both 80.0%. Multiple parallel simulations were carried out in the SWMM model, the simulated average values of TR-CR and PR-CR are 80.2% and 80.9%, respectively, which was close to the predicted value. The relative errors were 0.28% and 1.08%, respectively, indicating that the multiple quadratic regression model was reliable and suitable for this study.

Conclusions

(1) The sensitivity coefficients of area ratio, width, and soil hydraulic conductivity were higher among

the eight influencing factors, so the three factors were selected for the future simulation in the SWMM model of GR. The single-factor analysis and response surface analysis showed that all three factors significantly influenced the results. The order of influence on TR-CR and PR-CR were area ratio>hydraulic conductivity>width and area ratio>width>hydraulic conductivity, respectively.

(2) The relationships of area ratio, width, and soil hydraulic conductivity on TR-CR and PR-CR were established based on the RSM. The adj R^2 of the quadratic model were 0.9477 and 0.9871, respectively, which were well fitted with minor experimental errors and can be optimized for area ratio, width, and hydraulic conductivity, respectively.

(3) Based on the volume capture ratio of the annual rainfall of $70\% \leq \alpha \leq 85\%$ in Wuhu City, 80% was set as the control target in this study. The construction cost is the control target based on satisfying this volume capture ratio of annual rainfall. With an area ratio of 0.79, width of 2.21 m, and hydraulic conductivity of 55.59 mm/h, the mean simulated values of TR-CR and PR-CR were 80.2% and 80.9%, respectively. The relative errors were 0.28% and 1.08%, which indicated that the multiple quadratic regression model was reliable, so was determined as the optimal solution.

Acknowledgments

This work was supported by the Natural Science Foundation of Anhui Polytechnic University (Xjky2022172), the Provincial Quality Project of Anhui Higher Education Institution (2020jyxm0163), the General Natural Science Research Project of Higher Education Promotion Plan of Anhui Province (TSKJ2016B28), and the Undergraduate Science Research Program of Anhui Polytechnic University (2022DZ27).

Conflict of Interest

The authors declare no conflict of interest.

References

1. XING Y., SHAO D., LIANG Q., CHEN H., MA X., ULLAH I. Investigation of the drainage loss effects with a street view based drainage calculation method in hydrodynamic modelling of pluvial floods in urbanized area. *Journal of Hydrology*, **605**, 127365, **2022**.
2. XING Y., SHAO D., MA X., ZHANG S., JIANG G. Investigation of the importance of different factors of flood inundation modeling applied in urbanized area with variance-based global sensitivity analysis. *Science of the Total Environment*, **772**, 145327, **2021**.
3. DENG Z., WANG Z., WU X., LAI C., ZENG Z. Strengthened tropical cyclones and higher flood risk under

- compound effect of climate change and urbanization across China's Greater Bay Area. *Urban Climate*, **44**, 101224, **2022**.
4. ZHANG J. Effects of Low-Impact Development on urban rainfall runoff under different rainfall characteristics. *Polish Journal of Environmental Studies*, **28** (2), 7405, **2021**.
 5. HAMIDI A., RAMAVANDI B., SORIAL G.A. Sponge City – An emerging concept in sustainable water resource management: A scientometric analysis. *Resources, Environment and Sustainability*, **5**, 100028, **2021**.
 6. JIANG C., LI J., HU Y., YAO Y., LI H. Construction of water-soil-plant system for rainfall vertical connection in the concept of sponge city: A review. *Journal of Hydrology*, **605**, 127327, **2022**.
 7. ALIM M.A., RAHMAN A., TAO Z., GARNER B. GRIFFITH R., LIEBMAN M. Green roof as an effective tool for sustainable urban development: An Australian perspective in relation to stormwater and building energy management. *Journal of Cleaner Production*, **362**, 132561, **2022**.
 8. CRISTIANO E., URRU S., FARRIS S., RUGGIU D., DEIDDA R., VIOLA F. Analysis of potential benefits on flood mitigation of a CAM green roof in Mediterranean urban areas. *Building and Environment*, **183**, 107179, **2020**.
 9. JOHANNESSEN B.G., HAMOUZ V., GRAGNE A.S., MUTHANNA T.M. The transferability of SWMM model parameters between green roofs with similar build-up. *Journal of Hydrology*, **569**, 816, **2019**.
 10. BROEKHUIZEN I., SANDOVAL S., GAO H., MENDEZ-RIOS F., LEONHARDT G., BERTRAND-KRAJEWSKI J., VIKLANDER M. Performance comparison of green roof hydrological models for full-scale field sites. *Journal of Hydrology X*, **12**, 100093, **2021**.
 11. BAEK S., LIGARAY M., PACHEPSKY Y., CHUN J.A., YOON K., PARK Y., CHO K.H. Assessment of a green roof practice using the coupled SWMM and HYDRUS models. *Journal of Environmental Management*, **261**, 109920, **2020**.
 12. HAMOUZ V., MUTHANNA T.M. Hydrological modelling of green and grey roofs in cold climate with the SWMM model. *Journal of Environmental Management*, **249**, 109350, **2019**.
 13. RABBANI M., KAZEMI F. Water need and water use efficiency of two plant species in soil-containing and soilless substrates under green roof conditions. *Journal of Environmental Management*, **302**, 113950, **2022**.
 14. CAO J., HU S., DONG Q., LIU L., WANG Z. Green roof cooling contributed by plant species with different photosynthetic strategies. *Energy and Buildings*, **195**, 45, **2019**.
 15. JAHANFAR A., DRAKE J., GHARABAGHI B., SLEEP B. An experimental and modeling study of evapotranspiration from integrated green roof photovoltaic systems. *Ecological Engineering*, **152**, 105767, **2020**.
 16. CASCONI S., COMA J., GAGLIANO A., PÉREZ G. The evapotranspiration process in green roofs: A review. *Building and Environment*, **147**, 337, **2019**.
 17. STOVIN V., VESUVIANO G., KASMIN H. The hydrological performance of a green roof test bed under UK climatic conditions. *Journal of Hydrology*, **414-415**, 148, **2012**.
 18. LISENBEE W. A., HATHAWAY J. M., WINSTON R. J. Modeling bioretention hydrology: Quantifying the performance of DRAINMOD-Urban and the SWMM LID module. *Journal of Hydrology*, **612**, 128179, **2022**.
 19. SOULIS K.X., VALIANTZAS J.D., NTOULAS N., KARGAS G., NEKTARIOS P.A. Simulation of green roof runoff under different substrate depths and vegetation covers by coupling a simple conceptual and a physically based hydrological model. *Journal of Environmental Management*, **200**, 434, **2017**.
 20. BERGESON C.B., MARTIN K.L., DOLL B., CUTTS B. B. Soil infiltration rates are underestimated by models in an urban watershed in central North Carolina, USA. *Journal of Environmental Management*, **313**, 115004, **2022**.
 21. JENNETT T.S., ZHENG Y. Component characterization and predictive modeling for green roof substrates optimized to adsorb P and improve runoff quality: A review. *Environmental Pollution*, **237**, 988, **2018**.
 22. QUEZADA-GARCÍA S., ESPINOSA-PAREDES G., POLO-LABARRIOS M. A., ESPINOSA-MARTÍNEZ E. G., ESCOBEDO-IZQUIERDO M.A. Green roof heat and mass transfer mathematical models: A review. *Building and Environment*, **170**, 106634, **2020**.
 23. LIN Y., WU M., FANG F., WU J., MA K. Characteristics and influencing factors of heavy metal pollution in surface dust from driving schools of Wuhu, China. *Atmospheric Pollution Research*, **12** (2), 305, **2021**.
 24. CIPOLLA S.S., MAGLIONICO M., STOJKOV I. A long-term hydrological modelling of an extensive green roof by means of SWMM. *Ecological Engineering*, **95**, 876, **2016**.
 25. WEI T., JIM C.Y., CHEN A., LI X. Adjusting soil parameters to improve green roof winter energy performance based on neural-network modeling. *Energy Reports*, **6**, 2549, **2020**.
 26. SCOLARO T.P., GHISI E. Life cycle assessment of green roofs: A literature review of layers materials and purposes. *Science of the Total Environment*, **829**, 154650, **2022**.
 27. BABAEI S., GHAZAVI R., ERFANIAN M. Urban flood simulation and prioritization of critical urban sub-catchments using SWMM model and PROMETHEE II approach. *Physics and Chemistry of the Earth, Parts A/B/C*, **105**, 3, **2018**.
 28. NAGASE A. Novel application and reused materials for extensive green roof substrates and drainage layers in Japan – Plant growth and moisture uptake implementation –. *Ecological Engineering*, **153**, 105898, **2020**.
 29. LIU W., ENGEL B.A., FENG Q. Modelling the hydrological responses of green roofs under different substrate designs and rainfall characteristics using a simple water balance model. *Journal of Hydrology*, **602**, 126786, **2021**.
 30. PAITHANKAR D.N., TAJI S.G. Investigating the hydrological performance of green roofs using storm water management model. *Materials Today: Proceedings*, **32**, 943, **2020**.
 31. CHEN S., HU J., ZHANG Z., BEHRANGI A., HONG Y., GEBREGIORGIS A.S., CAO J., HU B., XUE X., ZHANG X. Hydrologic Evaluation of the TRMM Multisatellite Precipitation Analysis Over Ganjiang Basin in Humid Southeastern China. *Ieee Journal of Selected Topics in Applied Earth Observations and Remote Sensing*, **8** (9), 4568, **2015**.
 32. VIJAYARAGHAVAN K., REDDY D.H.K., YUN Y. Improving the quality of runoff from green roofs through synergistic biosorption and phytoremediation techniques: A review. *Sustainable Cities and Society*, **46**, 101381, **2019**.
 33. XIE H., LIU J. A modeling study of the interflow in the green roof. *Urban Forestry & Urban Greening*, **54**, 126760, **2020**.

-
34. SASHANK S., DINESH BABU P., MARIMUTHU P. Experimental studies of laser borided low alloy steel and optimization of parameters using response surface methodology. *Surface and Coatings Technology*, **363**, 255, **2019**.
 35. PENG Z., SMITH C., STOVIN V. The importance of unsaturated hydraulic conductivity measurements for green roof detention modelling. *Journal of Hydrology*, **590**, 125273, **2020**.
 36. YIN D., CHEN Y., JIA H., WANG Q., CHEN Z., XU C., LI Q., WANG W., YANG Y., FU G., CHEN A. S. Sponge city practice in China: A review of construction, assessment, operational and maintenance. *Journal of Cleaner Production*, **280**, 124963, **2021**.